Neural Networks and Particle Swarm Optimization Based MPPT for Small Wind Power Generator

Chun-Yao Lee, Yi-Xing Shen, Jung-Cheng Cheng, Yi-Yin Li and Chih-Wen Chang

Abstract—This paper proposes the method combining artificial neural network (ANN) with particle swarm optimization (PSO) to implement the maximum power point tracking (MPPT) by controlling the rotor speed of the wind generator. First, the measurements of wind speed, rotor speed of wind power generator and output power of wind power generator are applied to train artificial neural network and to estimate the wind speed. Second, the method mentioned above is applied to estimate and control the optimal rotor speed of the wind turbine so as to output the maximum power. Finally, the result reveals that the control system discussed in this paper extracts the maximum output power of wind generator within the short duration even in the conditions of wind speed and load impedance variation.

Keywords—Maximum power point tracking, artificial neural network, particle swarm optimization.

I. INTRODUCTION

THE advantages of small wind generator are small volume, easy installment, and little noise compared with other renewable energy sources. To increase the applicable wind power, the maximum power point searching and tracking is the major concern. Many MPPT studies has been proposed, such as, perturb and observe method, three-point-weighting comparison algorithm, and variable speed wind turbine power method, etc. The results demonstrated that the wind energy system is a nonlinear form, so it is difficult to establish the linear control method. The artificial neural network (ANN) is proposed to solve the nonlinear control problem. Since the control method is only investigated in the condition of fixed load impedance and there are only few studies concerning with both the conditions of wind speed and load impedance variation. Therefore, this study combines artificial neural network (ANN) with particle swarm optimization (PSO) to adjust the control parameters in conditions of wind speed and load impedance variations for MPPT.

C.-Y. Lee is with the Department of Electrical Engineering, Chung Yuan Christian University, Taoyuan County, Taiwan, 32023. (Phone: +886-3-265-4827; e-mail:CYL@cycu.edu.tw).
Y.-X. Shen, J.-C. Cheng, C.-W. Chang and Y.-Y. Li are with the Department of Electrical Engineering, Chung Yuan Christian University, Taoyuan County, Taiwan, 32023 (E-mail: g9778002@cycu.edu.tw).

II. THE STRUCTURE OF WIND POWER GENERATOR SYSTEM

For a typical wind power generator, the maximum power point can be found in the P_m-N curve, the output power and rotor speed characteristic curve, under a specific wind speed, as shown in Fig. 1. The maximum output power can be manipulated upon the control of the rotor speed of wind power generator, which means the output power will be raised from point B to point A [1] [2]. The structure of wind power system is shown in Fig. 2, where the motor's rotor speed of artificial wind field is controlled to simulate natural wind speed by using inverters. The coupling mode is adopted to drive the wind turbine with the permanent-magnet synchronous generator (PMSG) and the three-phase full bridge rectifier is connected to the generator's output terminal for providing load the DC source.
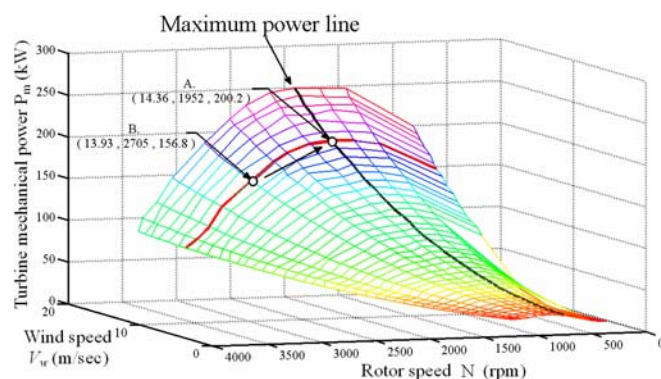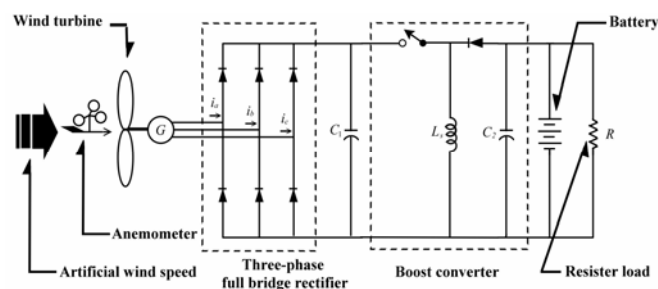

Fig. 1. Turbine power curves.

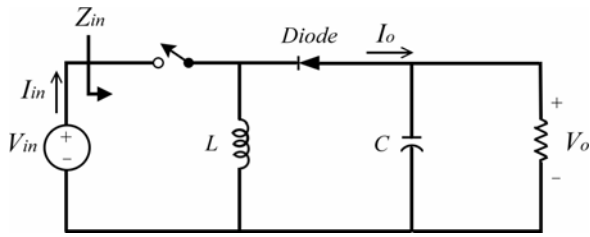Fig. 2. Structure of wind power system.

World Academy of Science, Engineering and Technology
International Journal of Electrical and Computer Engineering
Vol:3, No:12, 2009

Fig. 3. Boost converter circuit.

Fig. 3 demonstrates a structure of boost converter circuit. The equivalent impedance Z_{in} can be calculated by (1), where R is the impedance of converter output terminal. Since the rotor speed is influenced by Z_{in}, the maximum output power of generator is achieved by controlling duty cycle D.

$$Z_{in} = \frac{V_{in}}{I_{in}} = \frac{V_o(1-D)^2}{I_o} = R \cdot (1-D)^2 \qquad (1)$$

III. ARTIFICIAL NEURAL NETWORKS (ANN)

This study adopts back-propagation artificial neural network and its structure is multilayer feedforward network. The study uses the superiority of learning capacity to construct two estimation modules of artificial neural network, wind estimation ANN_{wind} and power estimation ANN_{Pe}, so as to estimate wind speed and output power. Many studies indicated that artificial neural network is available to approximate functions when the numbers of neurons are enough [3]. Therefore, the study firstly uses a hidden layer. To make the error within the tolerance, the number of neurons gradually increases until it achieves to a sufficient number. ANN_{wind} and ANN_{Pe} referring to two structures of multilayer feedforward neural network are applied to estimate wind speed and power respectively. Both of them correct the network weight by employing back-propagation algorithm. The training input and output of network will be illustrated in the following paragraph.
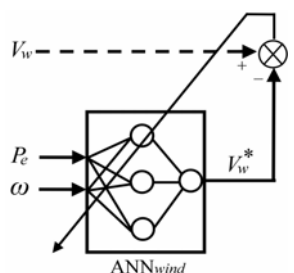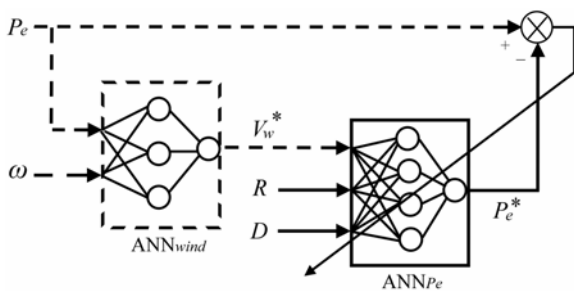

Fig. 4. Training scheme of ANN_{wind}.

Fig. 5. Training scheme of ANN_{Pe}.

The ANN_{wind} module is a 2 input - 1 output network structure, as shown in Fig. 4, where V_w is the actual wind speed by anemometer, P_e is the output power of generator, ω is the rotor speed of wind turbine, and V_w^* is the estimated wind speed by ANN_{wind}. The ANN_{Pe} module is a 3 input - 1 output network structure, as shown in Fig. 5, where R is load impedance, D is the duty cycle, and P_e^* is the estimated output power of generator by ANN_{Pe}. Moreover, P_e is not only the input signal of ANN_{wind} module but also the target in the training process of ANN_{Pe}. Therefore, before training the module of ANN_{Pe}, we must train the module of ANN_{wind} until the accurate rate of V_w^* achieves the expectation and then implement the training process of ANN_{Pe}.

IV. PARTICLE SWARM OPTIMIZATION (PSO)

PSO is a population-based searching algorithm. PSO randomly produces n_{popu} particles in searching space, and each particle includes position X_i and velocity V_i [4] [5], where X_i is the position of i-th particle in the searching space, $X_i =(X_{i1},…, X_{ij},…, X_{ik})$, and V_i is the velocity of i-th particle in the searching space, $V_i =(V_{i1},…, V_{ij},…, V_{ik})$. The position X_i of i-th particle represents a solution of the problem and the velocity V_i of i-th particle represents its displacement in the searching space. $Pbest_i$ is the optimal position that the i-th particle has experienced, and $pbest_i$ is the optimal fitness that the i-th particle has experienced. $Gbest$ is the optimal position that all particles have experienced and $gbest$ is the optimal fitness that all particles have experienced. When Fit(·) is the fitness function for solving the maximum value, the optimal position of each particle is shown in (2).

$$Pbest_i(t+1) = \begin{cases} Pbest_i(t) & \text{for } \text{Fit}(X_i(t+1)) \le \text{Fit}(Pbest_i(t)) \\ X_i(t+1) & \text{for } \text{Fit}(X_i(t+1)) > \text{Fit}(Pbest_i(t)) \end{cases} \quad (2)$$

To improve the convergence, $gbest$ and $Gbest$ are selected by comparing with the experiences of others. Therefore, the i-th particle is guided to three vectors (V_i, $Pbest_i$, and $Gbest$). The inertia weight method, shown as in (3) and (4), is applied to update velocity and position of the particles.

$$V_{ij}^{new} = w \cdot V_{ij} + c_1 \cdot rand1 \cdot (Pbest_{ij} - X_{ij})$$
$$+ c_2 \cdot rand2 \cdot (Gbest_j - X_{ij}) \qquad (3)$$

$$X_{ij}^{new} = X_{ij} + V_{ij} \qquad (4)$$

Where
$Pbest_i = (Pbest_{i1},…, Pbest_{ij},…, Pbest_{ik})$
$Gbest = (Gbest_1,…, Gbest_j,…, Gbest_k)$
$w = w_{max} - iter \cdot (w_{max} - w_{min})/iter_{max}$

c_1, c_2	acceleration coefficient
w	coefficient of the inertia weight
w_{max}	minimum coefficient of the inertia weight
w_{min}	maximum coefficient of the inertia weight
$iter$	current iteration number
$iter_{max}$	maximum iteration number

World Academy of Science, Engineering and Technology
International Journal of Electrical and Computer Engineering
Vol:3, No:12, 2009

Given the PSO method described above, the process of the PSO is shown as the following steps:

Step 1) Generate equivalent n_{popu} quantity of position and velocity randomly, and record $Pbest_i$, $pbest_i$, $gbest$, and $Gbest$.

Step 2) Calculate each fitness value of particles.

Step 3) If stopping criterion is satisfied (e.g., maximum iteration number), the procedure would go to the end; otherwise, proceed to step (4).

Step 4) Update the $Pbest_i$ and $pbest_i$.

Step 5) Update the $gbest$ and $Gbest$.

Step 6) Update particles position and velocity by applying (3) and (4), and then go back to step (2).

V. THE STRUCTURE OF MPPT CONTROL

The structure of MPPT control system is constructed by software and hardware communication environment through sensors and AD/DA cards. The process of MPPT control system is shown in Fig. 6, where the wind estimation ANN_{wind} and the estimated ANN_{Pe}-PSO of duty cycle are introduced as follows:

A. The Module of Wind Estimated ANN_{wind}

The use of sensors extracts the analog signals, V_o, I_o, and ω, where V_o and I_o are the output voltage and current of boost converter respectively. By applying AD/DA cards, the analog signals are transformed into digital signals which can be considered the input signals of ANN_{wind} for estimating wind speed and further delivering to ANN_{Pe}.

B. The Module of Duty Cycle Estimated ANN_{pe}-PSO

The application of sensors extracts the analog signals, voltage V_o and current I_o. The analog signals transform into the digital signals by applying AD/DA cards. The R, V_w^* and duty cycle (D_1, D_2,…,D_{sw}), are designated as the input signals of the ANN_{Pe}, where ANN_{Pe} is the fitness function Fit(·) of PSO for searching the optimal duty cycle D_{opt}.
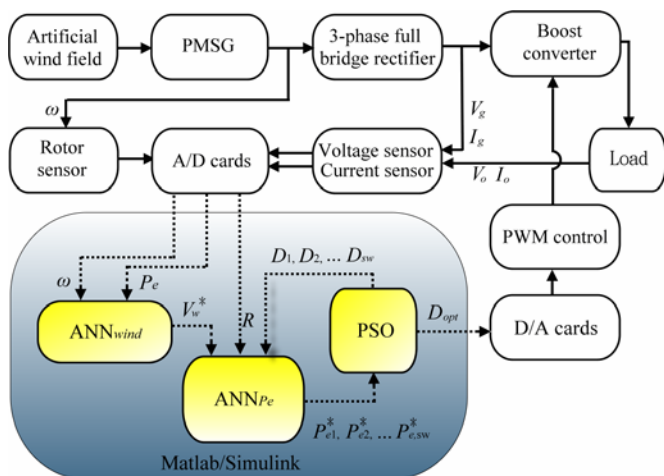

Fig. 6. Block diagram of the MPPT control System.

In the searching process, the control system initializes D_i and ΔD_i, and loads the signals P_e, ω and R. The signals, P_e, ω and R, are considered constants until the stopping criterion is satisfied and the control voltage V_{con} is delivered to PWM circuit, where V_{con} is the DC voltage level, 0~10V, for adjusting duty cycle. Subsequently, the MPPT control system adjusts duty cycle in order to reach D_{opt} by PWM circuit. Thus, the equivalent impedance makes the generator operate at the maximum power point. Where D_i, ΔD_i and sw are the positions of the i-th particle, the velocity of the i-th particle and the population size of PSO respectively. The output signals of ANN_{Pe}, P_{e1}^*, P_{e2}^*,…, $P_{e,sw}^*$, are the fitness of particle position, D_1, D_2,…, D_{sw}, respectively. The MPPT control system is accomplished by Matlab/Simulink, and the real-time control interface is shown in Fig. 7.

VI. EXPERIMENT RESULTS

A. The Module of Wind Estimated ANN_{wind}

The rotor speed, output power, and actual wind speed are gathered for training ANN_{wind}, and the trained result of ANN_{wind} is shown in Fig. 8. Therefore, the ANN_{wind} can estimate instantaneous wind speed because the estimated wind speed is adjusted along with the rotor speed and output power of generator. The ANN_{wind} can actually solve the problems of aging anemometer, placement movement, etc.
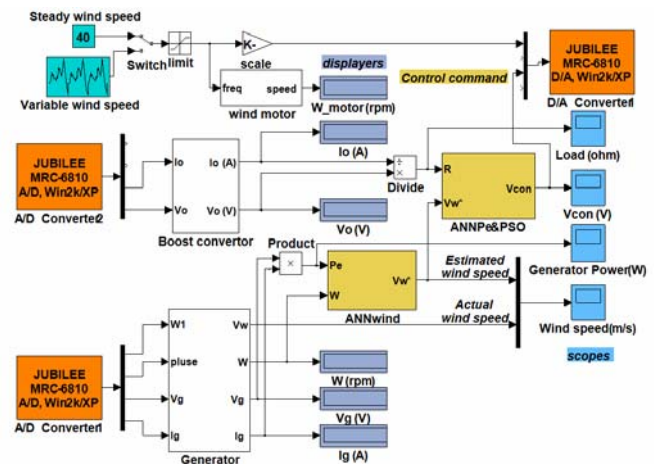
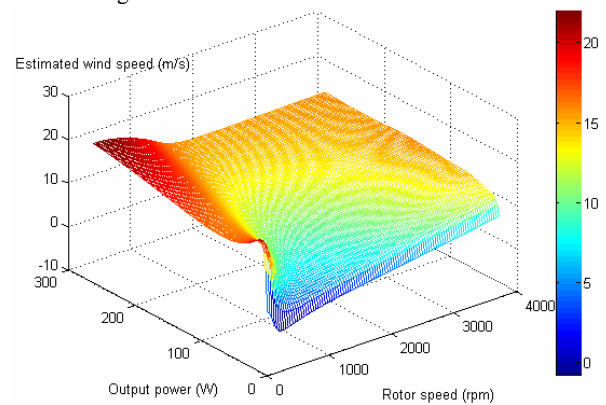

Fig. 7. Simulink structure of MPPT control.

Fig. 8. Three-dimensional curve of ANN_{wind}.

World Academy of Science, Engineering and Technology
International Journal of Electrical and Computer Engineering
Vol:3, No:12, 2009

B. The Module of Power Estimated ANN$_{Pe}$

The duty cycle, estimated wind speed, load impedance, and output power are gathered for training ANN$_{Pe}$, and the trained results of ANN$_{Pe}$ in the conditions of load impedance 50 (Ω) and 30 (Ω) are shown in Figs. 9 (a) and (b). The three-dimensional diagram reveals that the estimating wind speed, duty cycle, and output power are closely related. That is, each wind speed corresponds to one optimal duty cycle which generates the maximum power output in certain load impedance.

C. Maximum Power Point Tracking

For realizing the variation of output power in each wind speed, the load side connects to the 600 (W) variable wirewound resistor. The output power of generator against load impedance is shown in Fig. 10. The maximum output power is extracted under specific load impedance of different wind speeds. Therefore, the maximum powers can be regarded as expected values (38.6, 88.5, 167.5, 263.5 W) for specific wind speeds (7.6, 10.6, 13.0, and 15.0 m/s), according to Fig. 10. To observe the performance of MPPT control system, five experimental examples are designed and the effectiveness of the structure is discussed below.
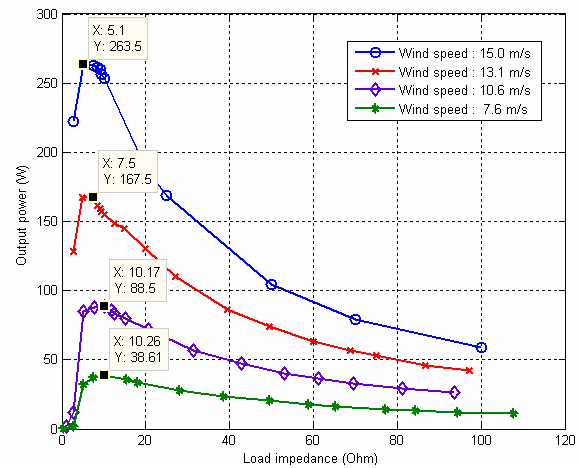

Fig. 10. The output power curves of generator.

1. Fixed Wind Speed and Load Impedance

Tables I and II demonstrates the results of MPPT in the conditions of the fixed load impedances (50 and 30 Ω) and fixed wind speeds (7.6, 10.6, 13.0, and 15.0 m/s). By comparing the expected values with output powers (actual values), the results reveal that the maximum absolute error is only 3.3 (%). Therefore, MPPT control system proposed in this paper is effective in the conditions of the fixed wind speed and load impedance.
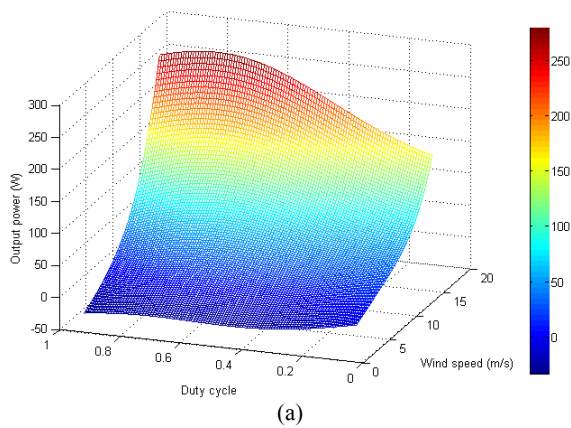
TABLE I
THE RESULTS OF MPPT IN THE CONDITION OF FIXED WIND SPEEDS (50 Ω)

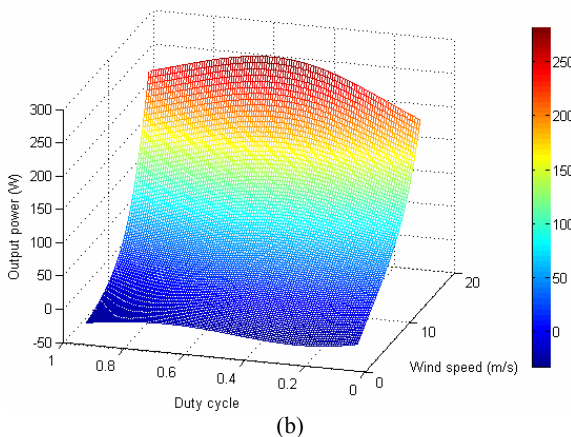| Wind speed (m/s)	Out power (W)		Absolute error (%)
	Expected value	Actual value	
7.6	38.6	**37.4**	**3.16**
10.6	88.5	**87.8**	**0.80**
13.0	167.5	**166.0**	**0.92**
15.0	263.5	**267.6**	**1.56**

TABLE II
THE RESULTS OF MPPT IN THE CONDITION OF FIXED WIND SPEEDS (30 Ω)

Wind speed (m/s)	Out power (W)		Absolute error (%)
	Expected value	Actual value	
7.6	38.6	**37.3**	**3.30**
10.6	88.5	**87.5**	**1.16**
13.0	167.5	**164.3**	**1.91**
15.0	263.5	**268.4**	**1.85**

2. Fixed Load Impedance and Sinusoidal Wind Speed

To observe the output power in the conditions of the regular wind speed variation and fixed load impedance, the inverter is controlled for sinusoidal wind speed variation (6~15 m/s), as shown in Fig. 11 (a), see solid line, and the load impedance is kept 50 (Ω), as shown in Fig. 11 (b). The estimated wind speed of the MPPT control system is also shown in Fig. 11(a), see dashed line. The estimated wind speed ignores small noise and tracks the sinusoidal variation, as shown in Fig. 11. In addition, the control voltage of the MPPT control system varies along with the estimated wind speed, as shown in Fig. 11 (c). Therefore, the rotor speed is adjusted by the MPPT control system due to V$_{con}$ variation. The result of MPPT reveals that the tendency of output power varying is similar to the

Fig. 9. Three-dimensional curve of ANN$_{Pe}$.
(a) Load impedance 50 Ω. (b) Load impedance 30 Ω.

World Academy of Science, Engineering and Technology
International Journal of Electrical and Computer Engineering
Vol:3, No:12, 2009

sinusoidal variation with delay phenomenon, as shown in Fig. 11(d). We record the instantaneous output powers of MPPT corresponding to the wind speeds (7.6, 10.6, 13.0 m/s) in Table III, where the absolute error indicates the error between expected value and average output power of rising and falling rotor speed. The result demonstrates that the output power has a temporary delay, that is, the output power is slightly smaller than the expected value while rotor speed rises, contrarily; the output power is slightly larger than the expected value while rotor speed falls. However, the maximum absolute error is only 4.83 (%), and the accumulated energy is nearly unvaried. The results discussed above revels that ANN$_{wind}$ can actually replace the anemometer, and MPPT control system can make generator operate at the maximum power point in this study.
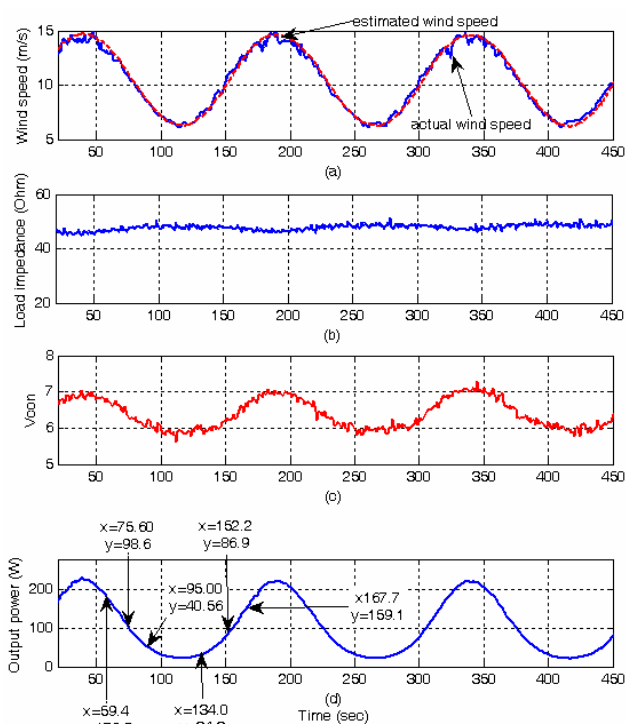

Fig. 11. MPPT result under sinusoidal wind speed and fixed load impedance.
(a) Wind speed. (b) Load impedance. (c) V$_{con}$. (d) Output power.

TABLE III
THE MPPT RESULT OF RISING AND FALLING ROTOR SPEED

From Table I.		From Fig. 11(d).		
Wind speed (m/s)	Expected value (W)	Out power (W)		Absolute error (%)
		Rising rotor speed	Falling rotor speed	
7.6	38.6	34.3	40.6	3.00
10.6	88.5	86.9	98.6	**4.83**
13.0	167.5	159.1	175.2	0.21

3. Fixed Load Impedance and Drastic Wind Speed Variation

To simulate the conditions of the fixed load impedance and drastic wind speed variation, the inverter is controlled for the step variation, as shown in Fig. 12 (a), see solid line, and the load impedance is kept 50 (Ω), as shown in Fig. 12 (b). When the wind speed (7.639 m/s) at 174.1 (sec) begins to increase

drastically, and reaches to 13.1 (m/s) at about 180.1 (sec), the estimated wind speed of the MPPT control system will rapidly track the actual wind speed, as shown in Fig. 12 (a), see dashed line. Therefore, before the estimated wind speed reaches to 13.1 (m/s) at about 186.3 (sec), the control voltage is adjusted upward rapidly due to the estimated wind speed, as shown in Fig. 12 (c). Based on the aforementioned depiction, the tracking time of MPPT control system is about 6.3 sec (186.3-180.1=6.3).

The result of output power with MPPT is shown in Fig. 12(d), and the average output powers of generator from 50 (sec) to 174.1 (sec) and from 186.3 (sec) to 250(sec) are shown in Table IV respectively. The result reveals that both averages are close to the expected values. Even if wind speed varies drastically, the wind power generator still extracts maximum output power within the short duration by the MPPT control system.
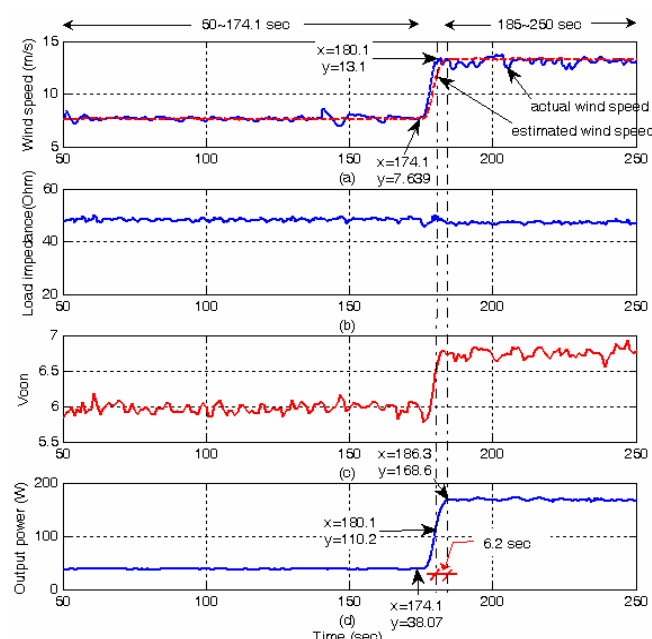

Fig. 12. MPPT under drastic wind speed and fixed load impedance.
(a) Wind speed. (b) Load Impedance. (c) V$_{con}$. (d) Output power.

TABLE IV
AVERAGE OUTPUT POWER IN CONDITION OF DRASTIC WIND SPEED VARIATION

Time range	Wind speed (m/s)	Expected power (W)	Average out power (W)	Absolute error (%)
50~174.1(sec)	7.6	38.6	37.8	2.07
186.3~250(sec)	13.0	167.5	168.3	0.45

4. Fixed Wind speed and Varied Load Impedance

The three different load impedances and the fixed wind speed are investigated. The estimated and actual wind speeds are shown in Fig. 13 (a). The load impedance is varied instantly from 48.38 (Ω) to 63 (Ω) and from 63 (Ω) to 27.32 (Ω) at 100.3 (sec) and 150.2 (sec) respectively, as shown in Fig. 13 (b). The control voltage will be adjusted while the load impedance varies by the MPPT control system, as shown in Fig. 13 (c). The w/ MPPT Line is the output power of generator without boost converter, and the w/o MPPT Line is the output power of generator with boost converter, as shown in Fig. 13 (d). The

World Academy of Science, Engineering and Technology
International Journal of Electrical and Computer Engineering
Vol:3, No:12, 2009

output power with MPPT control system hold on the maximum output power except the two instantaneous load impedance variations, as shown in Fig. 13 (d), see w/ MPPT Line. Moreover, as the load impedance varies, the two tracking times of MPPT control system are about 8.1 sec (108.4-100.3 = 8.1) and 8.7 sec (158.9-150.2 = 8.7). In addition, comparing the w/o MPPT Line with w/ MPPT Line, the average output powers are 48.9 (W) and 91.5 (W) respectively. The result reveals that the MPPT control system applied in this study improves the output power approximately 87%.
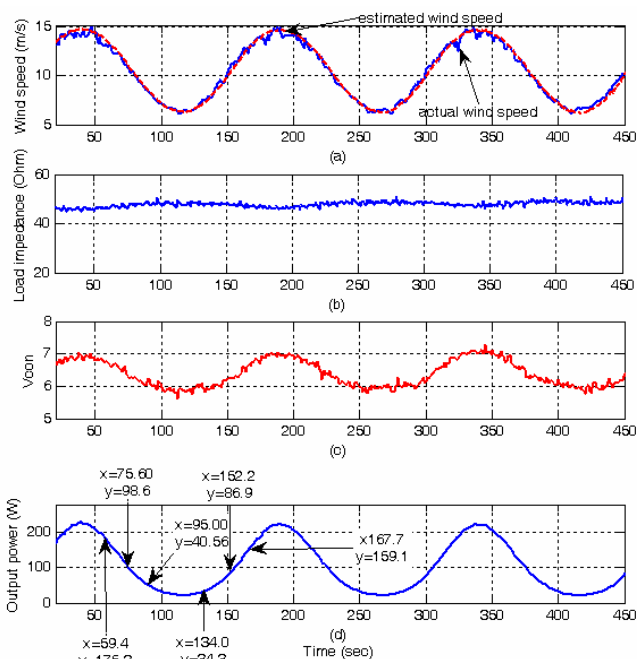

Fig. 13. MPPT under fixed load impedance and varied wind speed.
(a) Wind speed. (b) Load Impedance. (c) V_{con}. (d) Output power.

5. Varied Wind Speed and Load Impedance

To simulate the conditions of the wind speed and load impedance variations, the inverter is controlled for the arbitrary variation, as shown in Fig. 14 (a) , see solid line, and the load impedance varies instantly from 50.03 (Ω) to 23.22 (Ω) at 150 (sec), as shown in Fig. 12 (b). The control voltage of the MPPT control system varies along with the estimated wind speed and load impedance, as shown in Fig. 14 (c). The output power of MPPT is shown in Fig 14(d), see w/ MPPT Line. We record the instantaneous output powers of MPPT corresponding to the wind speeds (7.6, 10.6, 13.0 m/s) and load impedances (50.03 and 23.22 Ω) in Tables V and VI, where the absolute error indicates the error between the expected value and average output power of rising and falling rotor speed. The result demonstrates that the output power has temporary delay, and the maximum absolute error is only 8.70 (%).

Moreover, the MPPT result of Fig. 15 (a) is presented in Table I, and MPPT absolute error in condition of the fixed wind speed (10.6 m/s) is 0.80%. Thus, the tip speed ratio can be considered a basis of MPPT examination. On the other hand, the tip speed ratio in Fig. 15 (b) is almost the same with the tip speed ratio in Fig. 15 (a). Therefore, the MPPT control system

can make generator operate at the maximum power point even in the conditions of varied wind speed and load impedance. In addition, comparing the w/o MPPT Line with w/ MPPT Line, the average output powers are 60.5 (W) and 103.2 (W) respectively. The result reveals that the MPPT control system applied in this study improves the output power approximately 70%.
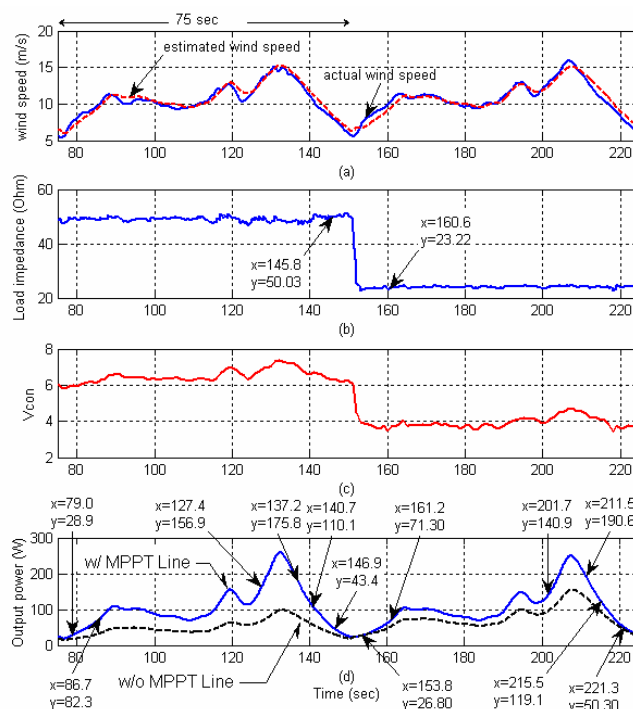

Fig. 14. Varied MPPT under wind speed and load impedance.
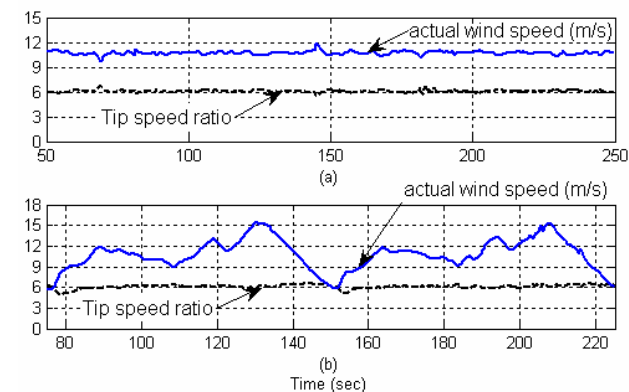(a) Wind speed. (b) Load impedance. (c) V_{con}. (d) Output power.

Fig. 15. Actual wind speed and tip speed ratio of (a)fixed wind speed and load impedance and (b) varied wind speed and load impedance.

TABLE V
THE MPPT RESULT AT THE RISING AND FALLING ROTOR SPEED (50.03 Ω)

From Table .I		From Fig.14 (d).		
Wind speed (m/s)	Expected power (W)	Out power (W)		Absolute error (%)
		Rotor speed rise (W)	Rotor speed fall (W)	
7.6	38.6	28.9	43.4	6.34
10.6	88.5	82.3	110.1	8.70
13.0	167.5	156.9	175.8	2.57

World Academy of Science, Engineering and Technology
International Journal of Electrical and Computer Engineering
Vol:3, No:12, 2009

TABLE VI
THE MPPT RESULT AT THE RISING AND FALLING ROTOR SPEED (23.22 Ω)

From Table I.		From Fig.14 (d).		
Wind speed (m/s)	Expected power (W)	Out power (W)		Absolute error (%)
		Rotor speed rise (W)	Rotor speed fall (W)	
7.6	38.6	**26.8**	**50.3**	**0.13**
10.6	88.5	**71.3**	**119.1**	**7.57**
13.0	167.5	**140.9**	**190.6**	**1.04**

VII. CONCLUSION

The control system based on Matlab/Simulink is applied to track the maximum power point of small wind power generator. The proposed ANN_{wind} estimates the instantaneous wind speed and ANN_{Pe} estimates output power of other rotor speed in a certain wind speed calculated by ANN_{wind}. The particle swarm optimization (PSO) plays an exploratory role for controlling the optimal rotor speed and further tracking the maximum power point. The effectiveness of the proposed approaches for maximum power point tracking (MPPT) is demonstrated with promising results. The ANN_{wind} not only replaces the measurement of anemometer but also solves the problems, such as, aging anemometer and moved position. Furthermore, the MPPT control system can extract the maximum output power within the short duration. The MPPT control system proposed in this paper can actually improve the effectiveness of small wind power generator in the conditions of wind speed and load impedance variations.

ACKNOWLEDGMENT

REFERENCES

[1] Hui Li, K. L Shi and P. G. McLaren, "Neuarl-Network-Based Sensorrless Maximum Wind Energy Capture With Compensated Power Coefficient," *IEEE Transaction on Industry Applications*. Vol. 41. No.6, November/December 2005.
[2] M. Veerachary, T. Senjyu, and K. Uezato, "Neural Network Based Maximum Power Point Tracking of Coupled Inductor Interleaved Boost Converter Supplied PV System using Fuzzy Controller," *IEEE Transactions on Industrial Electronics*, Vol. 50, No. 4, pp. 749-758, August 2003.
[3] Martin T. Hagan, Howard B. Demuth, Mark H. Beale, "Neural network design," University of Colorado Bookstore, 2002
[4] Clerc, Maurice," Particle Swarm Optimization," Paul & Co. Pub Consortium, 2006.
[5] J. Kennedy, R. Eberhart, "Particle swarm optimization," in *Proc. of IEEE International Conference on Neural Network*, vol. IV, Perth, Australia, pp. 1942-1948, 1995.

Chun-Yao Lee (S'05–M'08) received his Ph. D. in electrical engineering from Taiwan University of Science and Technology in 2007. During 2000-2007, he was a distribution system designer in the engineering division, Taipei Government. In August 2007, he joined Chung Yuan Christian University as a faculty member. He is presently an Assistant Professor. His major areas of research include power distribution and power filter design.

Yi-Xing Shen was born in Taiwan in 1986. He received his B.S. degree in electrical engineering from Chung Yuan Christian University in 2008. He is presently a graduate student toward his M.S. program in electrical engineering department of Chung Yuan Christian University in Taiwan.

Jung-Cheng Cheng was born in Taiwan in 1988. He is presently an undergraduate student toward his B.S. degree in electrical engineering department of Chung Yuan Christian University in Taiwan.

Yi-Yin Li was born in Taiwan in 1988. He is presently an undergraduate student toward his B.S. degree in electrical engineering department of Chung Yuan Christian University in Taiwan.

Chih-Wen Chang was born in Taiwan in 1988. He is presently an undergraduate student toward his B.S. degree in electrical engineering department of Chung Yuan Christian University in Taiwan.